AUTHOR(S):

TITLE:

YEAR:

Publisher citation:

OpenAIR citation:

Publisher copyright statement:

This is the _____ version of proceedings originally published by _____ and presented at _____ (ISBN _____; eISBN _____; ISSN _____).

This publication is distributed under a CC _____ license.

_____

Comparison of wear performance of thermal sprayed cermet (WC-Co) coatings from suspension and feedstock powders.

O. Ali [a], R. Ahmed [a], H. Alawadhi [b], M. Shameer [b], N.H. Faisal [c], N.M. Al-Anazi [d], M.F.A. Goosen [e]

[a] School of Engineering and Physical Sciences, Heriot-Watt University, Edinburgh, EH14 4AS, UK
[b] College of Sciences, University of Sharjah, P.O. Box: 27272, Sharjah, UAE
[c] School of Engineering, Robert Gordon University, Garthdee Road, Aberdeen, AB107GJ, UK
[d] Materials Performance Unit, Research & Development Centre, Saudi Aramco, Dhahran, 31311, Saudi Arabia
[e] Office of Research & Graduate Studies, Alfaisal University, P.O. Box 50927, Riyadh 11533, Saudi Arabia

WC-Co coatings were deposited using conventional High Velocity Oxy-Fuel Jet-Kote (HVOF-JK) and Suspension HVOF (S-HVOF) methods. Microstructural and mechanical properties along with the wear resistance of coatings were investigated. Reciprocating sliding wear tests were conducted against sintered Si_3N_4 counter-body with a normal load of 25N and total sliding distance of 500m following ASTM G133-2 standard. Coatings were characterised by Scanning Electron Microscope (SEM), X-Ray Diffraction (XRD) and nano-Indentation techniques. HVOF-JK coating showed good retention of WC whereas S-HVOF coating showed the presence of W, W_2C and amorphous/nanocrystalline phases. Nano-indentation of HVOF-JK and S-HVOF showed that the relative hardness of the HVOF-JK coating was higher but their elastic modulus was lower. The lower total wear rate was exhibited by the HVOF-JK coating. This difference in wear performance is attributed to the difference in hardness of the coatings and decarburisation of WC particles.

**Keywords**: Nanocomposite, sliding wear, suspension spray, tribology

1 Introduction

Thermal sprayed WC-Co coatings have been used for wear resistant applications in a number of industries such as aviation, aerospace, energy and power generation [1]. High Velocity Oxy-Fuel (HVOF) thermal spray process produces dense coatings with high hardness and good wear resistance when compared to plasma sprayed coatings. The wear resistance performance of coatings has been improving with decreasing Carbide Grain Size (CGS), due to the increase in hardness and the reduction of the mean free path which restricts crack propagation. An early investigation reported low wear resistance for nanostructured coatings (CGS was nano-scaled) due to severe decarburisation [2]. Since then nanostructured coatings have improved significantly, having better results than coatings with micro-scaled CGS, however inhomogeneous microstructure for the nano-coatings still poses problems. To produce more uniform and dense nanostructured coatings, WC-Co coatings are being produced using suspension solution by modifying existing HVOF and plasma systems for liquid feedstock. Investigations on the wear performance of Suspension HVOF (S-HVOF) have been performed previously and shown comparable wear performance to standard HVOF coatings under some tribological conditions [3-5]. In this study, a new S-HVOF coating is compared with a conventional HVOF coating in terms of wear performance, bulk mechanical and microstructural properties.

2 Experimental

2.1 Test materials

The conventional coatings are deposited using Jet Kote (HVOF-JK) thermal spray guns, details of which are given in a previous study [4]. For the S-HVOF coating a TopGun was modified for liquid feed injection. The aqueous suspension solution has 25% solid weight content. This weight content of WC-Co was based on a previous study [5]. The solid content of WC-12Co with nano-scaled carbides was supplied from GuangZhou, China. The powder was processed in a planetary ball mill before suspension solution preparation (shown in **Fig. 1.**) using the same method as used previously [3,4].
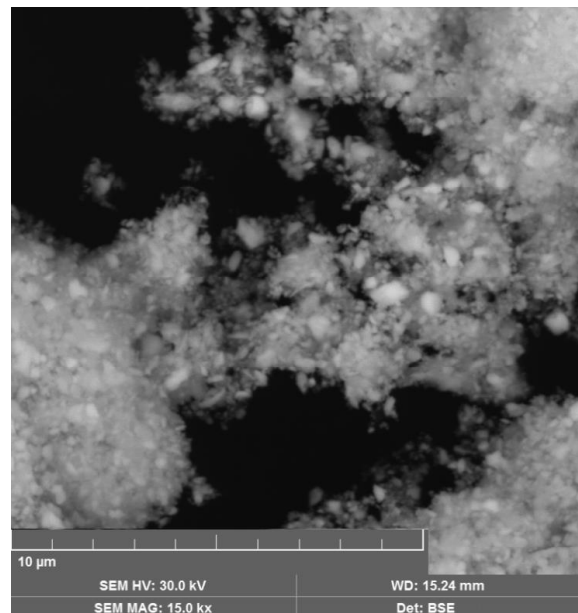
Fig. 1. SEM image of milled powder for S-HVOF.

2.2 Coating characterisation

Characterisation of coatings was conducted using Scanning Electron Microscope (SEM), X-Ray Diffraction (XRD), Energy Dispersive X-Ray Spectroscopy (EDX) and nano-indentation techniques. SEM was used to study the microstructural features of the polished cross-section of the coatings. A Bruker AXS, model D8 ADVANCE X-Ray diffractometer operating at 40kV and 40mA was used for XRD analysis, using Cu Kα radiation (wavelength λ=0.1542 nm). Nano-indentation was performed using a calibrated TriboIndenter® (Hysitron Inc., MN) equipped with Berkovich tip at the load of 50mN. Hardness and elastic modulus were calculated using the Oliver and Pharr method on coating cross-sections [6].
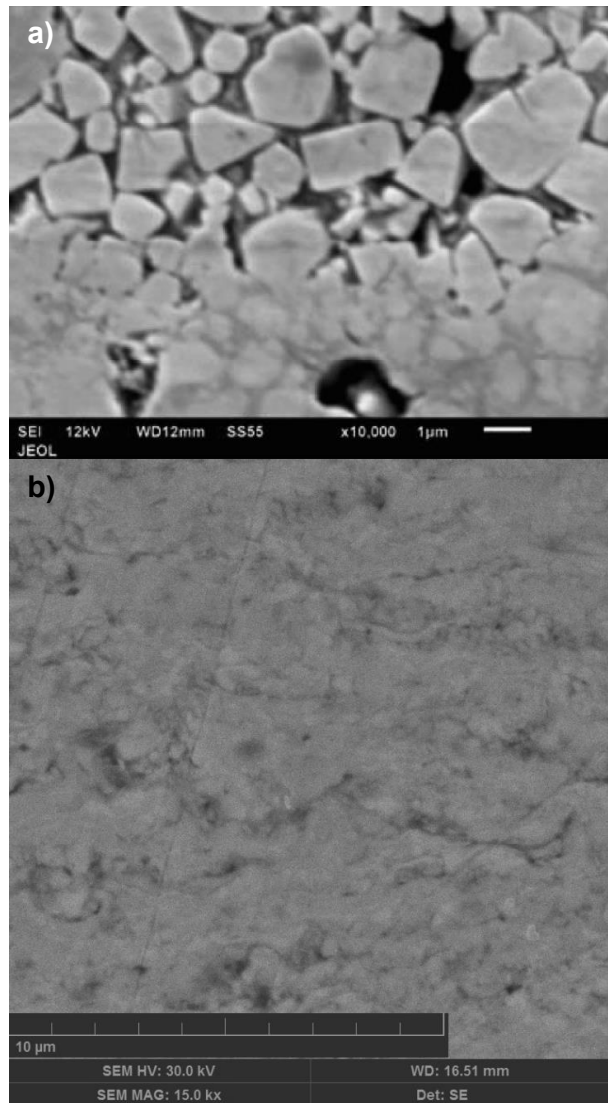
Fig. 2. SEM image of coating cross-sections of a) HVOF-JK [3] and b) S-HVOF (SE) coatings.

2.3 Sliding wear

Wear resistance of the coatings was tested under dry sliding conditions using ball-on-flat reciprocating sliding wear machine (BLR2000 M, Bud Labs, USA) at room temperature following ASTM G133-02 standard. The counter-body was sintered Si_3N_4 ball with diameter of 12.7mm (1/2 inch). The sliding distance was 500m with a normal load of 25N, reciprocating at 2Hz with a stroke length of 10mm. Sliding tests were repeated five times for each coating. Coating volume loss was measured from the average area of the wear track cross-section and the stroke length. The cross-section area was measured using interferometry (Zygo New View). Ball volume loss was measured using optical microscopy via the diameter of the wear scar on the ball. A tension-compression load cell loaded on the sliding wear machine was used to measure friction force to calculate the Coefficient of Friction (CoF). Wear tracks were analysed by use of SEM equipped with EDX, in Secondary Electron (SE) and Back Scattered Electron (BSE) modes to observe coating failure.

3. Results

3.1 Coating microstructure

Microstructural images obtained from the SEM are shown in **Fig. 2.** The HVOF-JK coating had a heterogeneous microstructure. The HVOF-JK coating had carbides which fused well with the Co matrix. The slightly rounded corners indicate that the solid carbide had slightly dissolved into the matrix [7]. S-HVOF coating had a lamella structure. Taking into consideration of thermal kinetics of suspension spraying method, some degree of decarburisation can be expected during coating deposition.
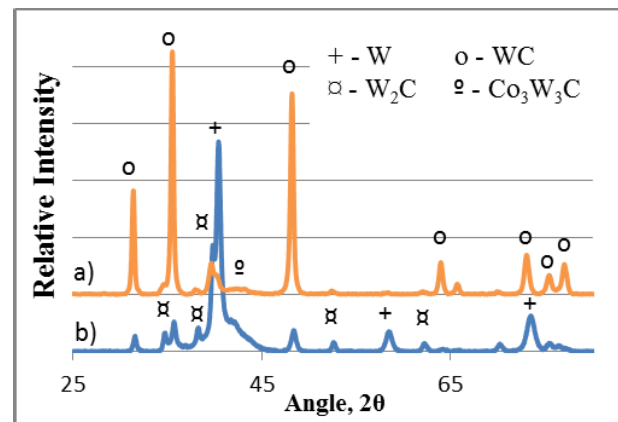
Fig. 3. XRD analysis of a) HVOF-JK [5] and b) S-HVOF coatings.
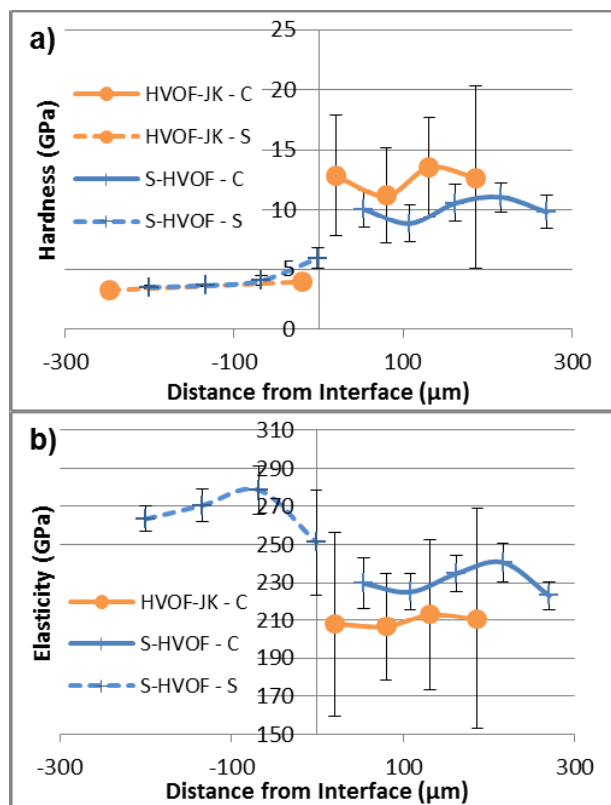
Fig. 4. a) Hardness and b) Elastic modulus from nano-indentation analysis of HVOF-JK [5] and S-HVOF coatings (C – Coating, S – Substrate).

In **Fig. 3.**, HVOF-JK coating showed limited decarburisation of WC with very limited amount of ternary η-phase (M_6C). S-HVOF coating showed relatively higher decarburisation of WC due to the presence of W and W_2C along with ternary η-phase. The hump, for values of 35-45 in 2θ, is indicative of the presence of amorphous/ nanocrystalline structures.

3.2 Nano-indentation analysis

Nano-indentation results of the coatings are compared in **Fig. 4.**, HVOF-JK coating results were performed in a previous study [5] and are compared with S-HVOF coating. HVOF-JK coating has higher hardness but lower elasticity than S-HVOF coating. The substrate for both coatings show a similar hardness.

3.3 Sliding wear test

The CoF of the sliding tests for each coating are shown in **Fig. 5a.**. The CoF for HVOF-JK were previously reported in another study [4]. The CoF of both coatings reached the same value at the end of the experiment at 500m, of roughly 0.55. The main difference between the coatings was the initial behaviour in the first 200m of the tests. HVOF-JK coating reached a stable value rapidly whereas the friction in the S-HVOF coating steadily increased with increasing sliding distance.
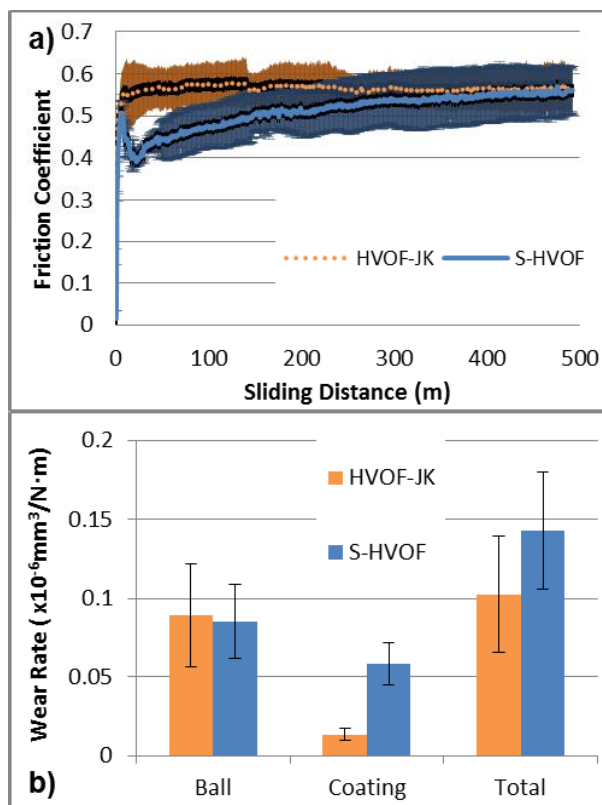
Fig. 5. a) CoF and b) Wear rate of ball, coating and total of all coatings sliding against Si_3N_4 ball for a distance of 500m.

HVOF-JK coating showed the highest wear resistance followed by the S-HVOF coating. The total wear rate was 0.10 ± 0.04 and 0.14 ± 0.04 ($x10^{-6}$ mm^3/N·m) for HVOF-JK and S-HVOF coatings, respectively. Ball, coating and total wear rates are shown in **Fig. 5b.** with respective standard deviation. SEM observation of the worn Si_3N_4 ball (S-HVOF test) is shown in **Fig. 6.** SEM image of the wear track of HVOF-JK is shown in **Fig. 7a.** and the wear track images of S-HVOF coating are shown in **Fig. 7b.** and **Fig. 7c.** The coatings showed no significant signs of tribofilm formation, except for the Si_3N_4 ball used against S-HVOF coating (see **Fig. 6.**). The tribofilms present on the ball contained W and Co along with increased O content. The debris collected from the sliding wear test of S-HVOF coating is shown in **Fig. 8.** The debris had flake-like morphology. The debris was mainly composed of W, O and C with varying levels of Si.
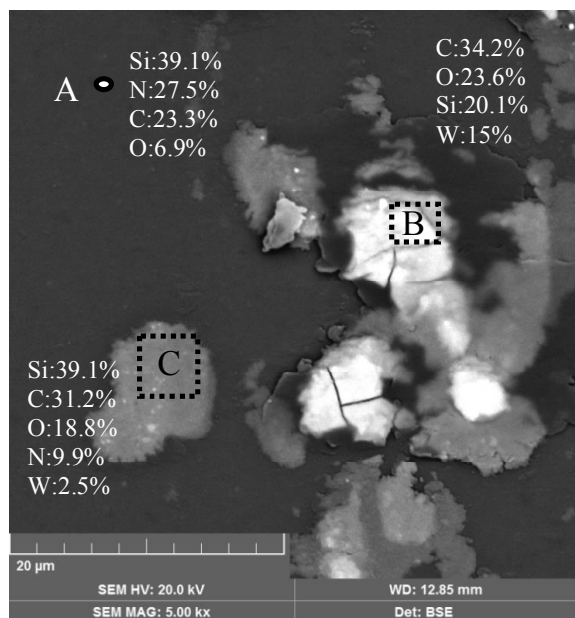
Fig. 6. Tribofilm formation on the ball for S-HVOF coating and EDX analysis of tribofilm deposited on the ball (A to C).

4. Discussion

4.1 Coating microstructure and properties

The microstructure of the HVOF-JK coating shows some signs of porous cavities while the S-HVOF has near negligible porosity. XRD analysis of HVOF-JK and S-HVOF coatings show very different microstructural phases. The larger carbides present in HVOF-JK coating are harder to melt when compared to nano-sized carbides present in the S-HVOF coating due to a relatively higher surface area to volume ratio, as described by Stewart et al. [8]. In previous studies of suspension coatings the decarburisation of WC has also been observed along with the presence of amorphous/nanocrystalline structures [3-5]. The decarburisation of WC in thermal process introduces W_2C, W and η-phase carbides in the coating microstructure. Wang et al. have suggested that this phenomenon is a combination of direct and indirect causes, the direct cause is melting of WC and indirect cause is the chemical interaction of molten Co during the deposition process [9].

4.2 Sliding wear performance

The ball wear rates of the two coatings are comparable but the respective coating wear rates had a significant difference in magnitude (see **Fig. 5b.**). The changes in the CoF are indicative of the transformation of the contact region in terms of contact area and is reflected in the coating wear rates.
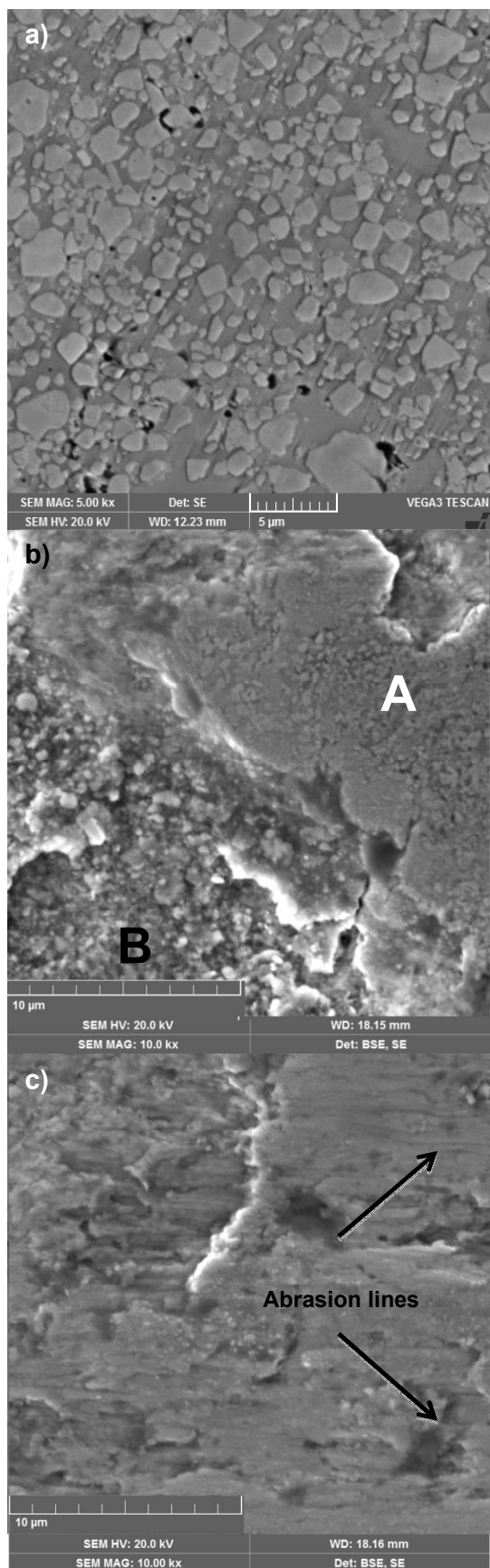
Fig. 7. Wear track SEM images of a) HVOF-JK, b) S-HVOF (A- shows matrix retention and B- shows delamination leading to exposed carbides) and c) S-HVOF coatings.

4.2.1 Coefficient of friction

The evolution of CoF with increasing sliding distance is linked to the changes in asperity interactions and the contact area of the ball. CoF for the S-HVOF coating starts off low as the asperities should be small due to the smaller carbides. Due to the higher extent of decarburisation the S-HVOF coating tends to be brittle with low toughness, especially the η-phase carbides [4]. This leads to high coating volume loss which leads to an increase in contact area causing the friction force to increase. The CoF of S-HVOF coating is plateauing at the end of the experiment, this means that the interactions are approaching a stable level. The continuous increase in contact area allows for the contact pressure to reduce. The high contact pressure combined with the brittle phases present could be a cause for the high S-HVOF coating wear rate. The conventional coating, HVOF-JK, reached stable CoF values earlier in the tests and respectively has a low coating volume loss.

4.2.2 Sliding wear observations and wear mechanisms

EDX analysis of the worn coating surfaces did not show major tribofilm formations or presence of elements originating from the ball. But a tribofilm formation was observed on the Si_3N_4 ball in the test against S-HVOF coating, which had increased content of W, Co and O. The formation and stability of this tribofilm (see **Fig. 6.**) can also be a contributing factor to plateauing of CoF curve as mentioned in the previous section. The wear track of the S-HVOF coating has signs of delamination and matrix retention, as shown in **Fig. 7b.** The cause for delamination is likely linked to the weak boundaries present in the microstructure of S-HVOF coating. In **Fig. 7c.** abrasion lines can be seen on the wear track of S-HVOF coating which is evidence that ploughing by the wear particles was taking place. The lack of tribofilm on the HVOF-JK coating has lead to matrix extrusion and carbide pull-out as the main method for volume loss (see **Fig. 7a.**). The low wear rate of the HVOF-JK coating can be attributed to the larger carbide size. Other factor contributing to the wear mechanism of both coatings included softening of the ball due to humidity in the air and tribo-chemical interactions in such an environment [10]. Ball wear rates for HVOF-JK and S-HVOF coatings are similar. In the case of S-HVOF coating the ball wear rate is high despite having tribofilm formed on the worn surface, this is attributed to the relatively lower hardness of the coating. The trapped debris contributed to 3-body abrasion and causes both the ball and coating to wear more than the HVOF-JK coating.

4.3 Role of microstructure in wear

The HVOF-JK coating has a blocky carbide microstructure, where the carbides were embedded well in the matrix and only get dislodged once the matrix has extruded sufficiently. This causes the ball wear rate to be high since no proper protective tribofilm is formed. The presence of weak boundaries in the microstructure of S-HVOF coating allows for the delamination in the coating, but the presence of region where matrix retention is occurring right alongside region of delamination indicate that once a splat has worn out, the contact pressure with relative motion causes the splat to delaminate and breakdown into fine debris (due to debris entrapment) which leads to 3-body abrasion. The maximum depth of S-HVOF coating wear tracks was on average 5.02μm compared to 1.19μm for HVOF-JK coating.

4.4 Debris morphology and role

The debris formed during the wear test of the S-HVOF coating (See **Fig. 8.**) has large flake-like morphology with some finer particles. There are two types of finer particles: ones which have an angular morphology which are likely to be formed due to the milling of the large flake-like debris and the other type of finer particles are the agglomeration of milled particles originating from the coating material. The second type of finer particles is formed due to debris entrapment and the subsequent 3-body abrasion taking place between the interacting surfaces. The flakes have one main source which is from the Si_3N_4 ball which has an increased content of Si. In **Fig.8.**, the EDX of point D has almost negligible Si content but a very high content of W. Comparing the EDX analysis of the tribofilm formed in **Fig. 6.** with the flakes in **Fig. 8.** (areas A-C in **Fig. 8.**), it can be seen that the tribofilm has higher Si content. This is due to the penetration effect of the EDX analysis, which also records the signal of the underlying material of the Si_3N_4 ball.
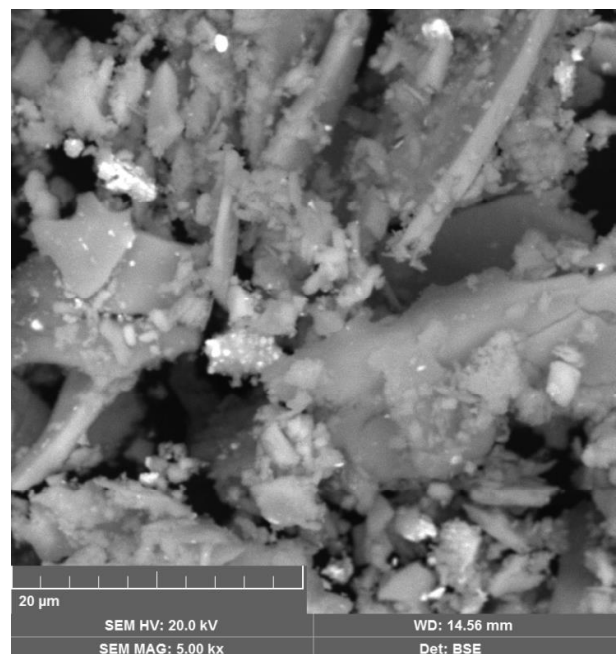

Fig. 8. SEM image of wear debris from sliding wear test of S-HVOF with EDX analysis.

5 Conclusion

1) Microstructural phases present in the microstructure of the S-HVOF coating were similar to the findings of previous study with the presence of η-phase ternary carbides and amorphous/nanocrystalline structures. Decarburisation of WC into W and W_2C was observed for S-HVOF coatings.

2) CoF of the coatings was almost the same for all coatings with differences in the evolution over the sliding distance.

3) Relatively lower hardness of the S-HVOF coating allows for easier removal of material causing the wear track depth to increase rapidly which conversely causes the respective ball wear rate to increase due to 3-body abrasion because of the entrapped debris.

4) Debris formed during the sliding wear test had multiple features originating from the coating and the ball. Debris formed from either origin showed distinct features.

6 References

[1]   Geng, Z., Li, S., Duan, D.L. and Y. Liu: Wear behaviour of WC-Co HVOF coatings at different temperatures in air and argon. Wear 330-331 (2015), pp. 348/53.

[2]   Qiao, Y, Fischer, T.E. and A. Dent: The effects of fuel chemistry and feedstock powder structure on the mechanical and tribological properties of HVOF thermal-sprayed WC-Co coatings with very fine structures. Surface and Coatings Technology 172 (2003), pp. 24/41.

[3]   Ali, O., Ahmed, R., Faisal, N.H., Alanazi, N.M., Berger, L.-M., Kaiser, A., Toma, F.-L, Polychroniadis, E.K., Sall, M., Elakwah, Y.O. and M.F.A. Goosen: Influence of Post-treatment on the Microstructural and Tribomechanical Properties of Suspension Thermally Sprayed WC–12 wt%Co Nanocomposite Coatings. Tribology Letters, 65 (2017) ,Issue 2, Art. No. 33.

[4]   Ahmed, R., Ali, O., Faisal, N.H., Al-Anazi, N.M., Al-Mutairi, S., Toma, F.-L., Berger, L.-M., Potthoff, A. and M.F.A. Goosen: Sliding wear investigation of suspension sprayed WC-Co nanocomposite coatings. Wear 322-323 (2015), pp. 133/50.

[5]   Ahmed, R., Faisal, N.H. , Al-Anazi, N.M., Al-Mutairi, S., Toma, F.-L, Berger, L.-M., Potthoff, A., Polychroniadis, E.K., Sall, M., Chaliampalias, D. and M.F.A. Goosen: Structure Property Relationship of Suspension Thermally Sprayed WC-Co Nanocomposite Coatings. Journal of Thermal Spray Technology 24 (2014), Issue 3, pp. 357/77.

[6]   Oliver, W.C. and Pharr, G.M.: An improved technique for determining hardness and elastic modulus using load and displacement sensing indentation experiments. Journal of Materials Research 7 (1992), issue 6, pp. 1564/83.

[7]   Ma, N., Guo, L., Cheng, Z., Wu, H., Ye, F. and K. Zhang: Improvement on mechanical properties and wear resistance of HVOF sprayed WC-12Co coatings by optimizing feedstock structure. Applied Surface Science 320 (2014), pp. 364/71.

[8]   Stewart, D.A., Shipway, P.H. and D.G. McCartney: Abrasive wear behaviour of conventional and nanocomposite HVOF-sprayed WC-Co coatings. Wear 225-229 (1999), pp. 789/98.

[9]   Wang, W., Xiang, J., Chen, G., Cheng, Y., Zhao, X. and S. Zhang: Propylene flow, microstructure and performance of WC-12Co coatings using a gas-fuel HVOF spray process. Journal of Materials Processing Technology 213 (2013), pp. 1653/60.

[10]   Dante, R.C. and C.K. Kajdas: A review and a fundamental theory of silicon nitride Tribochemistry. Wear 288 (2012), pp. 27/38.